Journal of Power Sources 189 (2009) 22–27

Contents lists available at ScienceDirect

Journal of Power Sources

journal homepage: www.elsevier.com/locate/jpowsour

Towards optimized preparation of cathode materials: How can modeling and concepts be used in practice

Miran Gaberscek

National Institute of Chemistry, Hajdrihova 19, SI-1000 Ljubljana, Slovenia

ARTICLE INFO

Article history:
Received 31 July 2008
Received in revised form 7 October 2008
Accepted 11 December 2008
Available online 24 December 2008

Keywords:
Cathode
Kinetics
Particle size
Coating
Porosity
Conductivity

ABSTRACT

A typical state-of-the-art Li cathode is a composite material consisting of many (nano) phases so its overall kinetics can be extremely sophisticated. In this paper we first show how one can identify selected important kinetic steps that may crucially affect the overall electrode performance. Based on relatively simple concepts supported with selected model experiments, we also give several practical recipes that might be helpful for designing of cathodes with improved overall kinetics.

1. Introduction

Many strategies that can lead to improved Li ion cathode performance have been reported: particle size minimization [1–4], introduction of controlled porosity [5,6], aliovalent doping [7,8], preparation of conductive matrices [9], preparation of conductive coatings [10,11], introduction of mixed conductors [12] and even introduction of ceramic coatings [13].

The abundance and diversity of these approaches may create an impression that there are many different problems that need to be addressed in a typical cathode. That transport inside a cathode can indeed be complex has been confirmed by extensive electrode modeling where a variety of possible transport and reaction steps have been identified [14–16]. However, it is accustomed in kinetic studies to focus primarily on the slowest steps because it is these that determine the overall rate. Thus, enhancing such steps will directly lead to enhancement of the overall transport.

The aim of the present work is to try to identify and discuss in some detail several possible rate-determining steps that may occur in a typical state-of-the-art cathode. The identification of the transport bottlenecks is based on combining the results of several carefully designed experiments and the results of our recent modeling of mass and charge transport on the continuum level. As shown in Section 4, at least for some cases quite clear picture emerges. It can be hoped that this clearer view will help experimentalists in future designing of cathodes with even better properties.

2. Theoretical

2.1. Dependence of electrode resistance on electrode mass

Let us divide the overall electrode kinetics in a typical electrode composite into three steps (Fig. 1a): (A) the transport of electrons and ions from their "reservoirs" to the active matter (e.g. active particles), (B) the charge incorporation reaction which involves the transfer of both charged species from the outside into the interior of active particles and (C) the transport of lithium component inside the solid active particles.

Case 1. Insertion of charge into active particles (step B and/or C) is much slower than transport of charge from reservoirs to the active particles (step A).

Here we follow the treatment introduced in our earlier paper [17]. Let the mass of one active particle be m_A and the number of such particles in an electrode N. If we neglect the additives, the electrode mass is given as $m_e = N \times m_A$. Let further the resistance of charge insertion (or deinsertion) into one particle be R_A. Then the resistance of insertion into N particles will be N-times smaller because their surface is N-times bigger):

$$R_{electrode} = \frac{R_A}{N} \text{ or equivalently } R_{electrode} = \frac{R_A m_A}{m_e} \quad (1)$$

E-mail address: miran.gaberscek@ki.si.

0378-7753/$ – see front matter © 2008 Elsevier B.V. All rights reserved.
doi:10.1016/j.jpowsour.2008.12.041

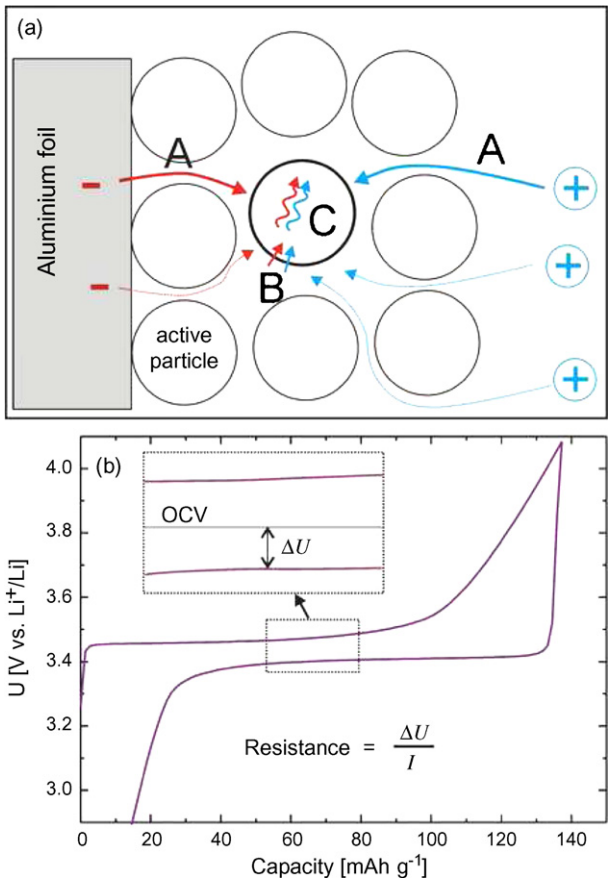

Fig. 1. (a) Schematical presentation of the division of overall electrode kinetics into steps A, B and C; (b) definition of electrode resistance used in the present paper.

This means that under the conditions above, the electrode resistance will be inversely proportional to the electrode mass (or to electrode thickness, if the surface area and the electrode density are constant).

Case 2. Insertion of charge into active particles (i.e., step B together with step C) is much faster than the transport from the reservoirs to the active particles (step A).

For easier treatment, we assume that the surface area of electrode, A, is constant so any increase in electrode mass will be exactly proportional to the increase in electrode thickness. The thicker the electrode, the longer will be the average paths for step A. So the electrode resistance will be proportional to the electrode thickness (or electrode mass):

$$R'_{electrode} = Km_e \tag{2}$$

where K is the proportionality constant.

2.2. Derivation of the electrode resistance for Case 1

Electrode resistance for the Case 1 above (see Section 2.1) can in some cases be analytically derived. More extensive derivation is reported in our previous papers [18,19], here we only repeat the main steps needed for Section 4. We start with a single particle. The particle is surrounded by an electronic and an ionic conductor. The rate-determining step for insertion/deinsertion is the solid state chemical diffusion within the particle. The surface reactions are assumed to be fast. Using the general equivalent circuit for transport in mixed conductors derived by Jamnik and Maier [20], we get for the impedance of the transport within the active particle the following expression:

$$Z = \frac{2}{d}\frac{1}{4\pi\sigma^\delta}\frac{1}{(d/2\sqrt{i\omega C^\delta/\sigma^\delta})\coth(d/2\sqrt{i\omega C^\delta/\sigma^\delta}) - 1} \tag{3}$$

where d is the particle diameter and ω is the angular frequency, while the total conductivity σ^δ is defined as

$$\sigma^\delta \equiv \frac{\sigma_{ion}\sigma_{electron}}{\sigma_{ion} + \sigma_{electron}} \tag{4}$$

where σ_{ion} and $\sigma_{electron}$ are ionic and electron conductivity of the particle, respectively. The chemical capacitance C^δ is defined as

$$C^\delta \equiv e^2\left(\frac{\partial\mu_{Li}}{\partial c_{Li}}\right)^{-1} \tag{5}$$

where e is the unit charge, μ_{Li} is the chemical potential and c_{Li} is the concentration of lithium in active particle. Extrapolating Eq. (3) to zero frequency, we get the resistance of active particle:

$$R_{part} = \frac{1}{10\pi d\sigma^\delta} \tag{6}$$

The total electrode resistance is obtained by summing up the contributions of all active particles constituting the electrode. Each particle is considered fully ionically and electronically wired. The total electrode resistance multiplied by mass of electrode, m_e, is then equal to the resistance of a single particle normalized per its mass:

$$R_{electrode}\cdot m_e = R_{part}v_0\rho = \frac{1}{60}\frac{\rho}{\sigma^\delta}d^2 \tag{7}$$

where v_0 is the particle volume and ρ is the particle density. The equality on the right was obtained by inserting Eq. (6). If m_e is transferred to the right side, we get the same dependence between the electrode resistance and mass as intuitively found in Eq. (1) (see Section 2.1).

Analogous treatment for the case of point contacting between the wire (coming from path A) and the surface of active matter, gives a cubic dependence between the electrode resistance and the particle diameter:

$$R_{electrode}\cdot m_e = \frac{\pi\rho}{12d_c\sigma_{chem}}d^3. \tag{8}$$

Again, if the particle size is constant, $R_{electrode}$ is inversely proportional to its mass, m_e.

3. Experimental

The experimental procedure is described in detail elsewhere [17]. Briefly, $LiFePO_4$/C composites were prepared by a citrate-based sol–gel method. Fe(III) citrate (Aldrich, 22,897-4) was dissolved in water at 60 °C. Separately, an equimolar water solution of LiH_2PO_4 was prepared from H_3PO_4 (Merck 1.00573) and Li_3PO_4 (Aldrich, 33,889-3). The sol obtained by mixing together the solutions was dried at 60 °C for at least 24 h. The obtained dried xerogel was fired in argon atmosphere for 10 h at 700 °C. The heating rate was 10 K min^{-1}. The final composite exhibited significant mesoporosity and, most importantly significant amount 3.5% of native carbon coating. The electrodes were prepared from this porous, carbon-coated material by casting and pressing a mixture of 84 wt.% of the as-synthesised material, 6.4 wt.% of carbon black (Printex XE2, Degussa) and 9.6 wt.% of a Teflon binder (Aldrich 44,509/6) on aluminium foil followed by drying at 110 °C for 24 h. The active material loading was from 1 mg cm^{-2} to 13 mg cm^{-2} corresponding to thickness of the active layer was from 30 μm to 90 μm. The geometric surface area of the working electrode was always 0.5 cm^2. The electrolyte used was a 1 M solution of $LiPF_6$ in EC:DMC (1:1 ratio by volume), as received from Merck. The electrochemical tests were

carried out in a laboratory-made three-electrode test cell. The working and the counter lithium electrodes were held apart with two separators (Celgard 2402) between which a thin strip of lithium serving as a reference electrode was positioned. The constant current during cell cycling was between 8.5 mA g^{-1} and 1700 mA g^{-1} (corresponding roughly from C/20 to 10 C, respectively).

4. Results and discussion

4.1. Determination of the slowest step in electrode kinetics

If we wish to enhance the overall transport, it is recommendable to first identify the slowest step and then try to make improvements in that particular step. For this purpose, we will here show two methods that are relatively easy to use in the battery research. Both methods rely on performing the most accustomed galvanostatic measurement but at different conditions.

The first method is based on the galvanostatic measurements at different currents I (given as A g^{-1}, in the battery community this current is usually given as C-rate). For each current (or C-rate) we determine the voltage polarization ΔU, which is defined as the deviation from the OCV (see the graphic representation in Fig. 1b). We then plot I as a function of ΔU (see Fig. 2a). A brief analysis of many literature data shows that the shape of this plot is quite general for most insertion batteries. Three regions can be distinguished,

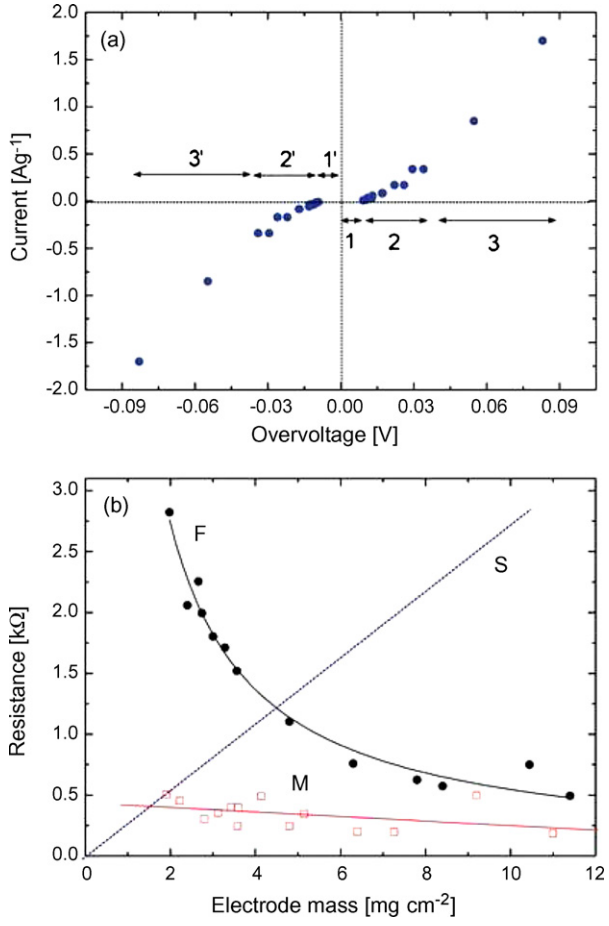

Fig. 2. (a) Current as a function of electrode polarization for carbon-coated porous $LiFePO_4$. The polarization was extracted from galvanostatic charge–discharge curves as schematically shown in Fig. 1b. The meaning of regions 1–3, etc. is explained in the text. (b) Three types of graphs obtained when measuring the dependence of electrode resistance on electrode thickness (or mass); points: actual measurements on LiFePO4 at C/10 (full circles) and at C/2 (open squares). Letters F, S and M are explained in the text.

as denoted in Fig. 2a. Most notably, there exists a polarization gap (region 1 or 1′), before current can start to flow. The reason for this is unknown and will have to be a subject of intensive further research. In any case, we can say, that one needs to invest some energy before the insertion process can start. In region 2 (or 2′) the current starts to flow and increases in an exponential fashion. In other words, at increasing overvoltage it becomes easier and easier for the current to flow. The impression is that the material becomes more and more activated. Later on (in region 3 or 3′), the current–polarization curve adopts a linear shape. In electrochemistry, the linear shape is characteristic for ohmic drops in the electrolyte, across contacts, etc. Our basic interpretation related to this fundamental curve is as follows: at low polarizations (region 2 or 2′), the current is determined by the process of insertion (steps B and C in Fig. 1a). At higher polarization the insertion becomes somehow activated and the current now becomes limited by the transport towards the active particles (step A)—that is why the current–voltage dependence becomes linear. So, in a given electrode different steps can be rate-determining, depending on the magnitude of polarization (or magnitude of current).

However, the rate-determining step should also depend on the electrode mass (or, more precisely, thickness). Imagine a very thick electrode in which the path for ions and electrons (step A) towards active particles positioned in the middle of electrode will be very long. Even if the ionic or electronic conductivity along path A is good (for example, if we have good electrode porosity and/or conductive coatings around the active material), the very long path will mean a high resistance for the whole step A. Eventually, at a certain thickness this resistance will become higher than the resistance due to insertion (steps B and C). The opposite will be true if the electrode mass (and hence the thickness) is small. This simple principle is the basis for the second method used in this paper for determination of the rate-determining step of an electrode. This method consists of measuring the galvanostatic curves for electrodes having different thicknesses. Because the electrode thickness is difficult to determine (it is merely several tens of micrometers), one can also measure the electrode mass which is proportional to the thickness—provided that the electrode area and density are kept constant. From the measured galvanostatic curves, one first determines the electrode resistance. This is simply obtained by dividing the electrode polarization with the galvanostatic current, i.e., $R_{electrode} = \Delta U/I$ (see Fig. 1b). Note that because the current is given in [Ag^{-1}], the unit for electrode resistance is [Ωg], that is, the usual resistance is here multiplied by mass unit. This is a sort of normalization which sometimes allows easier comparison between different electrodes. Note also that the same normalization was used in our derivation of Eqs. (7) and (8). Of course, we can also divide the electrode resistance by its mass and thus obtain the non-normalized electrode resistance. Exactly this is done in Fig. 2b, where the non-normalized electrode resistance is plotted as a function of electrode mass.

Three types of graphs are displayed in Fig. 2b. If the transport step A is fast compared to steps B and/or C (Case 1 in our theoretical treatment), then the type of curve denoted by F is obtained. This occurs at small polarization (region 2 or 2′ in graph 2a). Most importantly, the experimentally measured points exactly follow the corresponding theoretical prediction (the fit using either Eqs. (1), (7) or (8) is denoted by the solid curve). Once again, this confirms our hypothesis that at small rates the resistance due to insertion is much bigger than the resistance due to migration of ions and electrons along the path of step A. Interestingly, preliminary testing of TiO_2 anatase nanowire-like material showed that the F shape is preserved to C-rates as high as 10 C (in a sense, 10 C is percepted as low-rate for anatase material). We assume that due to their high aspect ratio, nanowire-like particles are more loosely packed than ordinary spheroidal particles. This way, nanowire-like particles can

accommodate more electrolyte which enhances the transport of ions towards TiO_2 up to relatively high rates. This indicates that quite big enhancement in the rate of step A is possible by certain morphological changes of active particles.

The other extreme theoretical case of transport limitation (Case 2, see Section 2.1) is demonstrated by curve S in Fig. 2b. Eq. (2) predicts a linear relationship between the electrode resistance and the electrode mass (or, in fact, thickness). We chose letter S to remind us that in this case the transport towards the active particles, i.e., step A, is slow if compared to steps B and C. This case is expected to occur at very high rates where the polarization curve becomes a completely straight line (ohmic drop completely prevails over the insertion). In terms of Fig. 2a, this would correspond to the end of region 3 or 3'. In any case, it is possible to predict that shape S will, generally, also occur in cases where the active particles are (very) small and/or possess a high chemical diffusion coefficient. Of course, curve S is also expected in cases where electrode porosity is insufficient (slowing down the transport of ions), where the amount of electronically conductive additive is too small, etc. Experiments to confirm this behaviour are underway.

The third typical case is the mixed-transport case exemplified by the experimental points along curve M in Fig. 2b. Again, these points correspond to measurement of coated $LiFePO_4$. Electrodes with different masses (thicknesses) were measured at C/2 and the resistance was determined as shown in Fig. 1b. At this rate, the kinetics due to transport step A are comparable to the kinetics due to steps B and/or C. In other words, this is an intermediate case between both extreme cases discussed above. It is thus not surprising that the inverse proportionality of curve F and the proportionality of curve S more or less annihilate and a very weak or even no dependence of $R_{electrode}$ on mass (or thickness) is obtained. We have experimentally observed this kind of curves for the aforementioned $LiFePO_4$ at C-rates slightly lower or higher than ca. C/2 and for TiO_2 anatase nanotubes at rates higher than ca. 30 C (not shown).

4.2. The effect of contacting between the electronic/ionic conductor and the active matter

In the theoretical part we showed that, besides the mass, the electrode resistance also depends on particles size and on the way how electronic and ionic paths are distributed immediately at the surface of active matter (Eqs. (7) and (8)). Speaking naively, this distribution determines how many electrons and ions per time unit can enter a given active particle. Depending on this distribution, two kinds of laws connecting electrode resistance and particle size can be predicted: a square law (Eq. (7)) and a cubic law (Eq. (8)). To easier understand the physical situation corresponding to both laws, we depicted the expected path of lithium insertion for both laws (Fig. 3a).

Comparing Eqs. (7) and (8), we realize that at a given particle size the electrode resistance will be much higher in the case of point contacting (Eq. (8)) than in the case of full contacting of both phases (Eq. (7)) around the particles (see Fig. 3, bottom). So, a good technology is such which not only minimizes the resistance of electronic and ionic paths leading towards the active particles but also minimizes the particle size and, at the same time, allows a full contacting of both phases around each active particle.

Of course, a full contacting of both phases around each active particle is the ideal situation which probably cannot be realized in most practical cases. Especially difficult is this realization when the particle size gets very small. From the many papers published in recent years (see Section 1), one gets an impression that there are many practical cases where one of the conductive phases forms a much better contacting with the active material than the other. In such "asymmetrical cases of contacting geometry", the ratio

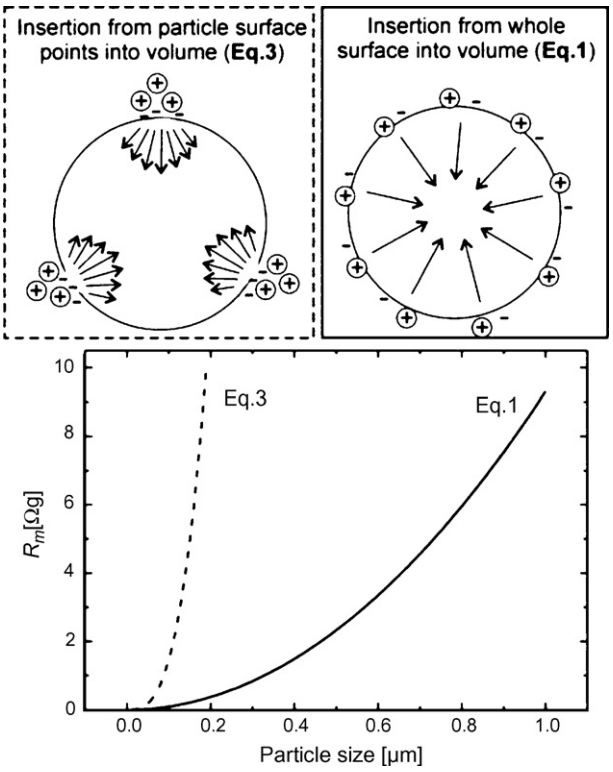

Fig. 3. Top: example of poor (left) and good (right) contacting between the ionic/electronic conductors and active particle. Bottom: corresponding calculated curves (using Eqs. (7) and (8)). In the calculation, the following values of parameters were used: $\rho = 3.5\,g\,cm^{-1}$, $\sigma_{ion} = 6.4 \times 10^{-11}\,S\,cm^{-1}$, $\sigma_{electron} = 3 \times 10^{-9}\,S\,cm^{-1}$, $d_{p.c.} = 20\,nm$, $n = 10$. Note that at any particle size the resistance due to point contacting is very much higher than that due to the whole-surface contacting.

between the ionic and the electronic conductivity of our active material becomes of crucial importance. Both asymmetrical cases are discussed in next two sections.

4.2.1. Electronic conductivity is much lower than ionic, $\sigma_{electron} \ll \sigma_{ion}$

Since the invention of $LiFePO_4$, basically all researchers have believed that this material satisfies perfectly the above criterion. This belief stemmed from the experimental fact that $\sigma_{electron}$ for $LiFePO_4$ was much lower (ca. $10^{-9}\,S\,cm^{-1}$ at RT) [7] than in most other materials used before (typically between $10^{-3}\,S\,cm^{-1}$ and $10^{-4}\,S\,cm^{-1}$ at RT [21,22]). Due to the arbitrary speculation that in $LiFePO_4$ $\sigma_{electron} \ll \sigma_{ion}$, many authors intuitively proposed various technological solutions to compensate for the apparently low electronic conductivity, such as aliovalent doping [7,8] or carbon coating technology [10,11]. While the true effect of aliovalent doping was later on disputed [23], the carbon coating strategy was quite generally accepted and, in a way, strengthened the belief that the identification of the problem ($\sigma_{electron} \ll \sigma_{ion}$) was correct and that the proposed solutions were conceptually sound. Only very recently, the actual effect of conductive coatings has been systematically investigated [3,19]. Our recent work [19], in fact, shows that the effect of conductive coating on the electrode resistance of $LiFePO_4$, if existent, is certainly much less important than the particle size effect. We explained this unexpected result by proposing that the basic assumption is actually reversed, that is that $\sigma_{electron} \gg \sigma_{ion}$. It seems that most previous authors mistakenly ascribed the good performance of their carbon-coated samples to the presence of carbon coating itself rather than to the fact that the presence of carbon suppressed the particle growth during material preparation.

Our opinion is that there are not many active materials where the above basic condition, $\sigma_{electron} \ll \sigma_{ion}$, is actually satisfied. But if we have to deal with such a material, then the coating strategy should indeed be helpful. The resistances of point-contacted and coated material should then roughly obey Eqs. (8) and (7) leading to the corresponding graphs in Fig. 3. Aliovalent doping which would increase $\sigma_{electron}$ should also be very effective in such cases.

4.2.2. Electronic conductivity is much higher than ionic, $\sigma_{electron} \gg \sigma_{ion}$

This case probably applies for most known battery materials, including $LiFePO_4$. Because here it is the ionic movement inside the active matter that is rate determining, we have to take care that as many as possible ions reach easily the surface of active particles. These, of course, have to be as small as possible to minimize the resistance according to Eqs. (7) and (8). But beside being small, the particles should also be sufficiently separated from each other to allow for full access of electrolyte (and thus ions) around each particle. It seems that while many authors put significant effort into particle size minimization, they pay much less attention to prevention of their agglomeration or even sintering. For example, one is often satisfied if the Scherrer's formula gives a small enough value for particle size; of course, this way the extent of particle agglomeration cannot be assessed.

According to our experience, prevention of particle agglomeration requires a special effort. In our most recent approach we achieved good results by using a silica precursor during heat treatment of a titania precursor [24]. The silica not only prevented excessive particle growth but also served as an inter-particle "spacer" in the final composite allowing for a better access of the electrolyte to the TiO_2 nanoparticle surface.

Another effective way in the battle against agglomeration is to use porous instead of particulate materials [5,6]. There the access of electrolyte will be controlled by pore size distribution and good pore-to-pore connectivity while the solid state diffusion rate will be determined by the thickness of walls between the pores.

How about the role of electron-conducting additives in cases where $\sigma_{electron} \gg \sigma_{ion}$? Are such additives necessary at all? As mentioned above, there is now not only theoretical but also experimental [3,19] evidence available that, in such cases, we certainly do no need to prepare special conductive coatings. But unless $\sigma_{electron}$ is by many orders of magnitude higher than σ_{ion}, it is easy to show that some conductive additive is still needed. Let us imagine the rather ideal situation depicted in Fig. 4, where the conductive additive surrounds a larger group of spherical active particles. The active particles are contacted in such a way that electrons can easily be transferred from one to another particle. At the same time, there is enough space in the inter-particle voids for accommodation of the electrolyte. Now, by analogy with Eq. (7) the ionic contribution to the electrode resistance will be determined by the particle dimension and its ionic conductivity [19]:

$$R_{particle,ionic} = \frac{1}{60}\frac{\rho}{\sigma_{ion}}d^2. \quad (9)$$

The electronic contribution within the given particle group, however, will depend on the average diameter of this group (because note that the electronic conductor is positioned around that group and there are no easy pathways for electron within the group). Again, by analogy with Eq. (7) we can estimate the electronic contribution to the electrode resistance by

$$R_{m,electronic} = \frac{1}{60}\frac{\rho_g}{\sigma_{electronic}}D^2, \quad (10)$$

where ρ_g is the average density and D the diameter of the group.

By comparing (4) and (5) we can get a rough criterion that tells us which is the maximum size of the group of particles that still causes no significant problems due to electronic conduction:

$$D \le d\sqrt{\frac{\rho}{\rho_g}\frac{\sigma_{electron}}{\sigma_{ion}}}. \quad (11)$$

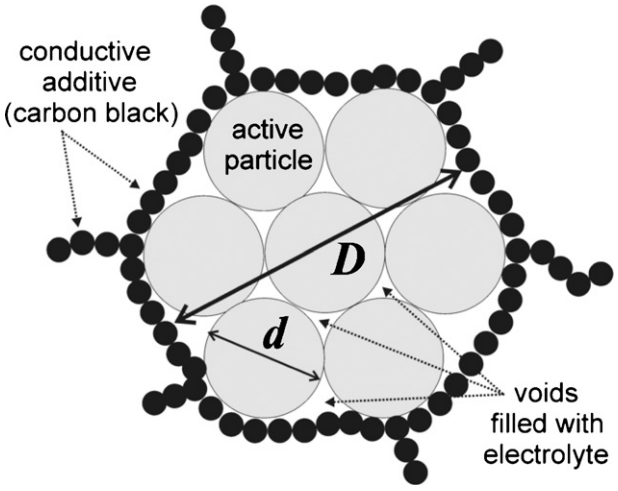

Fig. 4. Schematic visualization of the meaning of Eq. (11) (see the text). Of course, the real distribution of carbon black may deviate significantly from the pattern displayed, so Eq. (11) should be considered a rough approximation only.

As an example, let us use Eq. (11) for estimation of D in a $LiFePO_4$-based composite. Based on our previous estimations and on single crystal measurements, let us assume that in $LiFePO_4$ the ratio $\sigma_{electron}/\sigma_{ion}$ is in the order of 50. If we neglect the difference in the density of single particle and the group of particles, we find that $D \le 7d$. So, if the particle size of $LiFePO_4$ is about 100 nm, we need an electronically conductive additive to be distributed around clusters of particles that are no bigger than ca. 700 nm. Of course, such a relatively "mild" requirement can be satisfied by the usual addition of several wt.% of carbon black and its random distribution among the relatively big clusters of nanoparticles. Such simple ad-mixing of carbon black, however, could become problematic when D becomes comparable to the size of carbon black particles, e.g. below 200 nm; according to the present estimation this would happen when the particle size of $LiFePO_4$ becomes smaller than ca. 30 nm.

5. Conclusions

Some simple approaches for evaluation of the possible bottleneck processes in the Li cathode kinetics were presented. First we showed two methods that can distinguish between the transport of charges from their reservoirs (current collector, electrolyte) to the active particles and the further transport into and inside the active particles. The methods involve the usual measurement of galvanostatic charge–discharge curves at different C-rate or at different electrode thicknesses (or masses).

Particularly important for the kinetics is the way how the active particles are contacted by electronic and ionic conductor. We have presented a couple of simple criteria that determine the actual strategy towards optimization of this contacting. If the electronic conductivity of the active material is lower than the ionic, then the well known conductive coating strategy is recommendable. Alternatively, doping leading to conductivity enhancement can be used. However, in most active materials the ionic conductivity is actually lower than the electronic. In such cases we have to be particularly careful that after particle size minimization no particle agglomeration occurs. The use of special spacers could be a good approach. Alternatively, one can prepare porous particles with appropriate pore size distribution to enhance the ionic transport. Finally, we

presented a simple formula that can be used for a rough evaluation of the distribution of the electronically conductive additives (carbon black, etc.) needed for a good performance of composite electrodes.

Acknowledgements

The financial support from Slovenian Research Agency and the support from the European Network of Excellence 'ALISTORE' are acknowledged. The author also thanks M. Kuezma for carrying out both experiments shown in Fig. 2, and R. Dominko and J. Jamnik for fruitful discussions.

References

[1] M. Wagemaker, W.J.H. Borghols, F.M. Mulder, J. Am. Chem. Soc. 129 (2007) 4323.
[2] C. Jiang, M. Wei, Z. Qi, T. Kudo, I. Honma, H. Zhou, J. Power Sources 166 (2007) 239.
[3] C. Delacourt, P. Poizot, S. Levasseur, C. Masquelier, Electrochem. Solid State Lett. 9 (2006) A352.
[4] T. Drezen, N.M. Kwon, P. Bowen, I. Teerlinck, M. Isono, I. Exnar, J. Power Sources 174 (2007) 949.
[5] F. Jiao, A.H. Hill, A. Harrison, A. Berko, A. Chadwick, P.G. Bruce, J. Am. Chem. Soc. 130 (2008) 5262.
[6] R. Dominko, M. Bele, J.M. Goupil, M. Gaberscek, D. Hanzel, I. Arcon, J. Jamnik, Chem. Mater. 19 (2007) 2960.
[7] S.Y. Chung, J.T. Bloking, Y.M. Chiang, Nat. Mater. 1 (2002) 123.
[8] G.X. Wang, S.L. Bewlay, K. Konstantinov, H.K. Liu, S.X. Dou, J.H. Ahn, Electrochim. Acta 50 (2004) 443.
[9] H. Huang, S.C. Yin, L.F. Nazar, Electrochem. Solid State Lett. 4 (2001) A170.
[10] N. Ravet, Y. Chouinard, J. Magnan, S. Besner, M. Gauthier, M. Armand, J. Power Sources 97 (8) (2001) 503.
[11] R. Dominko, M. Bele, M. Gaberscek, M. Remskar, D. Hanzel, S. Pejovnik, J. Jamnik, J. Electrochem. Soc. 152 (2005) A607.
[12] Y.S. Hu, Y.G. Guo, R. Dominko, M. Gaberscek, J. Jamnik, J. Maier, Adv. Mater. 19 (2007) 1963.
[13] C. Li, H.P. Zhang, L.J. Fu, H. Liu, Y.P. Wu, E. Rahm, R. Holze, H.Q. Wu, Electrochim. Acta 51 (2006) 3872.
[14] D. Dees, E. Gunen, D. Abraham, A. Jansen, J. Prakash, J. Electrochem. Soc. 152 (2005) A1409.
[15] V. Srinivasan, J. Newman, J. Electrochem. Soc. 151 (2004) A1517.
[16] Y.-H. Chen, C.-W. Wang, G. Liu, X.-Y. Song, V.S. Battaglia, A.M. Sastry, J. Electrochem. Soc. 154 (2007) A978.
[17] M. Gaberscek, M. Kuzma, J. Jamnik, Phys. Chem. Chem. Phys. 9 (2007) 1815.
[18] M. Gaberscek, J. Jamnik, Solid State Ionics 177 (2006) 2647.
[19] M. Gaberscek, R. Dominko, J. Jamnik, Electrochem. Commun. 9 (2007) 2778.
[20] J. Jamnik, J. Maier, Phys. Chem. Chem. Phys. 3 (2001) 1668.
[21] H. Tukamoto, A.R. West, J. Electrochem. Soc. 144 (1997) 3164.
[22] J. Guan, M. Liu, Solid State Ionics 110 (1998) 21.
[23] N. Ravet, A. Abouimrane, M. Armand, Nat. Mater. 2 (2003) 702.
[24] B. Erjavec, R. Dominko, P. Umek, S. Sturm, A. Pintar, M. Gaberscek, Electrochem. Commun. 10 (2008) 926.